


# Alzheimer's Detection in 3D Magnetic Resonance Imaging Using Deep Convolutional Neural Networks

Augusto Berwaldt de Oliveira   [ Federal University of Rio Grande do Sul | [augusto.oliveira@inf.ufrgs.br](mailto:augusto.oliveira@inf.ufrgs.br) ]

Claudio Resin Geyer  [ Federal University of Rio Grande do Sul | [geyer@inf.ufrgs.br](mailto:geyer@inf.ufrgs.br) ]

 Institute of Informatics, Federal University of Rio Grande do Sul (UFRGS), Av. Bento Gonçalves, 9500, Porto Alegre, RS, 91501-970, Brazil.

Received: 12 July 2025 • Accepted: 15 February 2026 • Published: 27 April 2026

**Abstract.** Alzheimer's disease (AD) is a progressive neurodegenerative disorder that affects millions of people worldwide and poses significant challenges for early and accurate diagnosis. In this paper, we present a comparative study between two-dimensional (2D) and three-dimensional (3D) convolutional neural networks (CNNs) for Alzheimer's disease detection using T1-weighted magnetic resonance imaging (MRI). A robust preprocessing pipeline based on the MNI-152 atlas is employed, including spatial normalization, skull stripping, and intensity normalization, ensuring anatomical consistency across subjects. A key contribution of this work is the adaptation of transfer learning from 2D to 3D CNNs, achieved by volumetrically extending pretrained 2D convolutional filters to initialize 3D kernels, improving convergence and feature representation in volumetric models. The proposed approach is evaluated on 2,603 MRI volumes from the ADNI dataset using a controlled experimental setup with identical preprocessing, training, and validation procedures for both models. Experimental results show that the 2D CNN achieved higher classification accuracy (90.17%) compared to the 3D CNN (87.88%), while both approaches demonstrated strong potential for MRI-based AD detection. These findings provide practical insights into the trade-offs between slice-based and volumetric CNN architectures in neuroimaging applications.

**Keywords:** Machine Learning, Alzheimer, Computer Vision, Deep Learning, Image Processing, CNN, MRI

## 1 Introduction

Alzheimer's disease (AD) is an irreversible neurological disorder characterized by dementia, leading to the loss of cognitive functions such as memory, orientation, attention, and language, ultimately impairing the ability to perform even the simplest tasks. It typically manifests in middle to old age and is characterized by the accumulation of proteins within and around neurons Lakhan *et al.* [2024]. One of the earliest and most common symptoms of AD is difficulty remembering new information, as the disease often starts in the areas of the brain responsible for learning. Additional symptoms may include behavioral changes, profound confusion about time, events, and places, as well as uncertainty about the identity of family members and friends. These symptoms progress gradually, leading to worsening memory loss and significant challenges with swallowing, speaking, and walking Guo *et al.* [2022].

Over the past two decades, extensive research has been conducted to detect Alzheimer's disease (AD) using artificial intelligence techniques. Machine learning algorithms, such as neural networks and support vector machines (SVMs), have been widely applied to analyze brain imaging data, including positron emission tomography (PET) and magnetic resonance imaging (MRI) Kazemi and Houghten [2018]. However, the detection of AD presents significant challenges due to low image quality, issues with brain segmentation and preprocessing, the lack of sufficiently large databases, and the inherent complexity of medical images. Effective classification requires a robust ability to identify distinguishing features in

similar brain images Qin *et al.* [2022].

A systematic literature review demonstrated that deep learning models consistently outperform traditional machine learning approaches in Alzheimer's disease detection. Among the 114 studies analyzed, 18 directly compared both paradigms, providing strong evidence of the superior performance of deep learning techniques. Based on these findings, this study focuses exclusively on the investigation and comparative analysis of deep learning models, as reported by Lakhan *et al.* [2023].

The advancement of graphics processing units (GPUs) has significantly supported the development of innovative deep learning algorithms. As a specialized subset of machine learning, deep learning mimics the human brain's ability to process data and recognize patterns, enabling solutions to complex decision-making tasks Shen *et al.* [2017]. These approaches have enhanced intelligent systems across various domains, including the analysis of medical images. Among deep learning models, convolutional neural networks (CNNs) have revolutionized disease detection and organ segmentation Ebrahimighannavieh *et al.* [2020]. Unlike traditional machine learning methods, CNNs integrate feature extraction, feature selection, and classification into a single framework. Recent studies indicate that CNNs are the most frequently used method accounting for approximately 70% of AD detection efforts Litjens *et al.* [2017].

MRI has emerged as the most widely used biomarker for AD detection in deep learning research, featuring in over 80% of studies employing single-modal approaches. This paper aims to classify AD patients and normal controls (NCs) using

MRI scans analyzed through CNNs Pradhan *et al.* [2024]. Our goal is to utilize CNNs to extract latent representations, identify relationships among image slices, and detect patterns indicative of AD in brain scans. A key contribution of this research is the expansion of transfer learning concepts from two-dimensional (2D) to three-dimensional (3D) MRI data, enabling the transfer of learnable parameters from 2D CNNs to 3D CNNs Pradhan *et al.* [2024].

The paper begins by reviewing related work, detailing the structure of CNNs and the application of 2D and 3D CNNs for AD detection through neuroimaging. Various types of CNNs, with and without transfer learning, are then examined for managing MRI volumes. Next, we present our proposed deep learning model, which introduces transfer learning to 3D CNNs. Finally, we discuss the experimental results and conclude with insights into the implications and potential of this approach. The main contributions of this work are as follows:

- **A systematic comparison between 2D and 3D CNN models** for MRI-based Alzheimer's disease detection, using identical preprocessing, training configurations, and validation procedures to ensure a fair and controlled evaluation.
- **A robust preprocessing pipeline based on the MNI-152 atlas**, enabling consistent anatomical alignment, skull-stripping, and normalization, which improves data quality for deep learning-based classification.
- **A novel adaptation of transfer learning from 2D to 3D CNNs**, achieved by volumetrically extending pre-trained 2D filters to initialize 3D convolutional kernels, improving convergence and feature extraction in 3D architectures.
- **An extensive evaluation using 2,603 MRI volumes from the ADNI dataset**, ensuring methodological rigor, reproducibility, and alignment with state-of-the-art neuroimaging studies.
- **Experimental evidence demonstrating the performance differences between 2D and 3D CNNs**, showing that the 2D approach achieved higher accuracy (90.17%) compared to the 3D model (87.88%), despite the richer volumetric representation learned by 3D networks.

The remainder of this paper is organized as follows. Section 2 reviews recent studies related to Alzheimer's disease detection using deep learning and neuroimaging. Section 3 presents the theoretical background and describes the CNN architectures and algorithms relevant to this work. Section 4 details the materials and methods, including dataset description, preprocessing steps, and the design of the 2D and 3D CNN models. Section 5 reports and discusses the experimental results obtained from both approaches. Finally, the last section provides concluding remarks and outlines future directions for improving MRI-based Alzheimer's detection. This table 1 allows us to compare.

## 2 Related Works

The growing prevalence of Alzheimer's disease (AD) and the demand for early and accurate diagnosis have motivated

extensive research into automated detection methods. With the increasing availability of medical imaging data—particularly magnetic resonance imaging (MRI)—deep learning has emerged as a powerful tool for analyzing complex brain patterns associated with neurodegeneration. In this context, numerous studies have proposed machine learning and, more recently, deep convolutional neural network (CNN) architectures to classify and monitor AD progression. This section reviews recent efforts in the use of CNNs for Alzheimer's detection, highlighting the main approaches, datasets, and techniques that have shaped the field.

The integration of artificial intelligence (AI) techniques into medical practice has led to substantial advancements in the diagnosis and prognosis of various diseases, with particularly notable results in MRI-based diagnostics. A recent systematic review by Zhang and Qie (2023) highlights that deep learning (DL) models can achieve diagnostic performance comparable to, or even surpassing, that of experienced clinicians across several imaging modalities, including X-ray, computed tomography (CT), and magnetic resonance imaging (MRI) Zhang and Qie [2023]. Among DL approaches, convolutional neural networks (CNNs) have demonstrated strong effectiveness in MRI classification tasks, such as brain tumor detection Dorfner *et al.* [2025] and cardiac disease recognition Wolterink *et al.* [2017]. Moreover, the use of pre-trained CNN architectures—such as ResNet, DenseNet, MobileNet, and ShuffleNet—has become increasingly common for feature extraction. These models are valued for their ability to adapt efficiently to new medical imaging tasks, often requiring less training data while maintaining high predictive accuracy Dorfner *et al.* [2025].

Qin *et al.* (2022) propose an innovative approach using Graph Convolutional Networks (GCNs) to assist in Alzheimer's disease diagnosis based on resting-state fMRI (rs-fMRI) Qin *et al.* [2022]. Their method constructs a brain functional network graph where nodes represent regions of interest (ROIs) and edges represent functional connectivity. Using data from 91 subjects in the ADNI dataset—44 diagnosed with AD and 47 cognitively normal—the authors developed a U-shaped GCN (U-GCN) model. Performance was compared to standard CNN methods and alternative GCN architectures such as GraphSAGE, TAGCN, and higher-order GNNs. The U-GCN outperformed all competing models, achieving an accuracy of 83.33%, sensitivity of 88.89%, and specificity of 77.78%. Interestingly, the study also highlights that, unlike traditional CNNs, deeper GCNs do not necessarily yield improved results, likely due to overfitting or reduced global representational capacity.

Feng *et al.* (2019) introduce a novel deep learning framework, termed FSBi-LSTM, which combines a 3D convolutional neural network (3D-CNN) with a fully stacked bidirectional LSTM (FSBi-LSTM) for Alzheimer's disease diagnosis using MRI (and PET) imaging Feng *et al.* [2019]. In this architecture, FSBi-LSTM replaces the conventional fully connected (FC) layer, enabling the preservation of rich spatial information from the 3D-CNN feature maps. The method captures structural dependencies across feature map slices more effectively than traditional SBi-LSTM models, which tend to collapse spatial structure via FC layers. The approach was validated on the ADNI dataset, where it achieved impressive

**Table 1.** Comparative summary of related studies and the proposed work.

Study	Data Modality	Preprocessing	Model Type	Transfer Learning	Key Contribution	Accuracy
Qin et al. (2022)	rs-fMRI	ROI graph construction	U-shaped GCN	No	Graph-based functional connectivity modeling for AD detection	83.33%
Feng et al. (2019)	MRI / PET	Standard MRI preprocessing	3D-CNN + Bi-LSTM	Partial	Sequential structural feature modeling using FSBi-LSTM	89.72%
Ebrahimi-Ghahnavieh et al. (2019)	MRI	Normalization + skull stripping	2D-CNN	Yes (2D)	Transfer learning applied to MRI slices for AD classification	85–89%
<b>Present Study</b>	MRI (3D T1)	<b>MNI-152 normalization + skull stripping</b>	2D-CNN / 3D-CNN	<b>Yes (2D → 3D)</b>	<b>Novel transfer learning application to 3D CNNs and full comparison of 2D vs. 3D models</b>	<b>90.17% / 87.88%</b>

performance metrics—an accuracy of 89.72%, sensitivity of 86.36%, and specificity of 65.35%—surpassing competing CNN and GNN based models Feng *et al.* [2019].

The problem of class imbalance in medical data mining arises when skewed class distributions introduce bias during model training, disproportionately affecting minority classes often associated with critical disease states. Salmi et al. (2024) provide a comprehensive review of the last decade's approaches to address this challenge, classifying them into data-level preprocessing techniques, algorithm-level modifications, and hybrid methods Salmi *et al.* [2024]. Similarly, Lopes et al. (2024) highlight the importance and effectiveness of such strategies in medical imaging contexts, showing improved detection rates by combining sampling methods and cost-sensitive learning Lopes *et al.* [2024]. These findings emphasize that without adequate handling of imbalance, predictive models perform poorly on underrepresented cases, even when overall accuracy remains high.

In summary, the literature reveals a growing interest in the application of ensemble models for MRI-based classification, particularly in differentiating between various stages of dementia, including Alzheimer's disease. Nonetheless, several challenges remain to be addressed, such as the need for robust validation of these models across diverse and heterogeneous clinical datasets. This is essential to ensure their generalizability and practical effectiveness in real-world diagnostic settings.

### 3 Background and Algorithms

When inputs are provided in vector form, as seen in many algorithms utilizing multi-layer perceptrons, vectorization disrupts the structural information of surrounding voxels or pixels in images. In contrast, convolutional neural networks (CNNs) are widely regarded as the most effective deep learning models for image analysis. Inspired by the visual cortex of the brain, CNNs are specifically designed to capture the spatial relationships within images by stacking multiple convolutional layers to extract increasingly abstract features Bhatt *et al.* [2021].

Unlike multi-layer neural networks, CNNs have significantly fewer parameters due to shared weights in convolutional layers and the use of pooling layers. Although CNNs showed promise early on, their widespread application has only become feasible in recent years with the development of innovative techniques and advanced computer systems for efficient training Sulam *et al.* [2019]. CNNs gained substantial recognition after their success in the ImageNet competitions, where they excelled in classifying a database containing approximately one million images across 1,000 distinct categories Yu *et al.* [2017].

This section provides an overview of the foundational concepts, architectures, and applications of CNN models in the context of Alzheimer's disease detection.

#### 3.1 CNN Architecture

A CNN (Convolutional Neural Network) is a type of neural network designed to analyze image-based data by automatically identifying patterns such as edges, textures, shapes, and

objects. It works by applying convolutions that extract important features without requiring manual preprocessing. In computer vision, CNNs are essential for tasks like image classification, object detection, segmentation, facial recognition, and medical image analysis, as they deliver high accuracy by learning directly from data and interpreting images in a way that resembles the human visual system.

A typical convolutional neural network (CNN) is composed of multiple layers, including convolutional layers, activation layers, pooling layers, fully connected layers, and a final Sigmoid layer. Training a CNN involves two main steps: a forward pass, where the model computes the loss by comparing the predicted outputs with the ground-truth labels, and a backward pass, which adjusts the learnable parameters based on the loss using a penalization method.

The performance of a CNN largely depends on its architecture and the configuration of its filters, which has driven researchers to explore and design various architectures to enhance performance Mutasa *et al.* [2021]. We can see examples of CNNs in Figure 1. This section explains the key components that form the foundation of a CNN architecture.

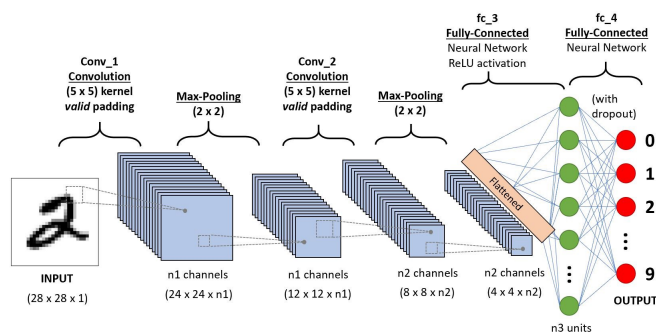


Figure 1. CNN Example

### 3.1.1 Convolutional layers

The convolutional layer is the foundational layer in a CNN architecture. It performs the convolution operation on an input image using a kernel, producing feature maps. The initial convolutional layers in deep CNNs extract discriminative, scale-invariant, and shift-invariant features from local regions of the image. Meanwhile, the later convolutional layers utilize these extracted features for task-specific classification Chauhan *et al.* [2018].

A significant advantage of convolutional layers is the concept of weight sharing within the same feature map, which reduces the number of parameters and simplifies the model while maintaining its effectiveness Chauhan *et al.* [2018].

### 3.1.2 Activation layers

A non-linear activation function, such as Sigmoid, Tanh, or ReLU, is typically applied after convolutional layers to generate a feature map for each filter. Introducing non-linearity enables the model to learn complex representations. Historically, activation functions like Sigmoid were widely used, but their saturation property often hindered the efficiency of learning algorithms during neural network training Hao *et al.* [2020].

To address this issue, ReLU emerged as a popular alternative and has been widely adopted in most studies. ReLU applies an element-wise activation function defined as  $\max(0, x)$ , offering significantly faster training times compared to Sigmoid and Tanh. Despite its advantages, ReLU can lead to zero gradients for negative input values, which can hinder learning. To overcome this limitation, Leaky ReLU was introduced, modifying the function to output  $0.01 \times x$  for  $x < 0$  instead of forcing all negative values to zero Billones *et al.* [2016].

### 3.1.3 Pooling layers

A pooling layer is a third type of layer typically positioned after convolutional layers in a CNN. It downsamples the input feature map by replacing each region with either its average or maximum value. Pooling reduces the number of parameters in the network while preserving the most significant features Bringas *et al.* [2020].

Historically, average pooling was commonly used; however, it has been largely supplanted by max pooling in recent years Karwath *et al.* [2017]. Max pooling has demonstrated faster convergence, improved classification performance, and better generalization by selecting superior invariant features.

### 3.1.4 Max-Pooling Layer

Max-Pooling is a common operation in convolutional neural networks (CNNs) used to reduce the spatial dimensionality (height and width) of feature maps, while retaining the most important information Tolia *et al.* [2015]. This technique helps to reduce computational cost, control overfitting and highlight the most relevant patterns Wu and Gu [2015].

The benefits of Max-Pooling include the prevention of overfitting, as it reduces the complexity of the model, preventing it from over-fitting the training data. It also reduces dimensionality, reducing the amount of data processed in subsequent layers and making the model more efficient. Another advantage is the invariance to small translations, allowing the CNN to recognize similar characteristics, even if they are slightly displaced, which improves the network's ability to generalize Zafar *et al.* [2022].

### 3.1.5 Fully connected layers

The fourth type of layer in a CNN is the fully connected layer, which functions similarly to traditional neural networks. It contains a significant portion of the learnable parameters in the network. After the feature maps have been processed through the previous layers, they are flattened into a vector, losing their spatial arrangement. The fully connected layer is then applied, linking each element of the vector to the corresponding features of the previous layer Liu *et al.* [2018]. These layers help to model non-linear relationships among the local features extracted by the convolutional layers.

## 3.2 Sigmoid layer

At the output layer, the sigmoid function plays a crucial role in binary classification problems by producing probabilities. Its output, ranging from 0 to 1, can be interpreted as the

likelihood of a given instance belonging to a specific class. The Sigmoid function is used for the classification of two classes, commonly known as binary classification Mesran *et al.* [2024]. The Sigmoid function is given by

$$\sigma'(x) = \sigma(x)(1 - \sigma(x))$$

### 3.3 CNN Models in Research Studies

Since the early 2010s, solving the computer and machine vision problems using CNN techniques has been gaining momentum Ebrahimighahnavieh *et al.* [2020]. Several computer vision problems are image classification, image segmentation, object detection, feature extraction, and object tracking. Deep learning methods for detecting Alzheimer's disease (AD) through neuroimaging are broadly classified into unsupervised and supervised approaches. Unsupervised models focus on deriving abstract representations from imaging data, typically using an autoencoder (AE) for feature extraction, followed by a support vector machine (SVM) for classification Guo [2017]. In contrast, supervised methods, which dominate the literature, combine feature extraction and classification into a single, integrated process. Among these, convolutional neural networks (CNNs) are the most widely adopted models for AD detection in advanced deep learning systems.

Some studies prioritize designing custom CNN architectures. However, leveraging well-established structures like AlexNet Irfansyah *et al.* [2021], LeNet Kayed *et al.* [2020], VGGNet Muhammad *et al.* [2018], GoogLeNet Szegedy *et al.* [2015], ResNet He *et al.* [2016], DenseNet Carcagni *et al.* [2019], and Inception Szegedy *et al.* [2017] can be highly beneficial. These models have demonstrated success in image classification tasks, as evidenced by previous research and ImageNet competitions.

## 4 Materials and Methods

This section provides a detailed account of the experimental data and the tools utilized for implementing the MRI image classification method. It also outlines the pre-processing steps applied to the images to enhance their effectiveness during classifier training. Finally, it describes the CNN models, both 2D and 3D, employed for testing and training purposes.

Figure 2 illustrates the block diagram of an AD detection system. The preprocessing phase includes steps such as intensity normalization, registration, and tissue segmentation, which prepare MRI scans for input into intelligent systems. Once preprocessing is complete, the MRI data is further organized and formatted to align with the structure of each implemented deep learning model.

Figure 2. The block diagram of an AD detection system.



Data management methods include slicing 3D MRI scans into 2D images, identifying regions of interest (ROIs), extracting 2D or 3D patches, and resizing. This study implements three approaches for AD detection using CNNs. In the slice-based approach, 2D image slices are extracted from 3D MRI

scans and processed using a 2D CNN as the deep learning model.

### 4.1 Image acquisition

The ADNI dataset, 3D T1-weighted MRI scans were acquired in digital imaging and communications in medicine (DICOM) format using Siemens (49.23%), GE (29.74%), and Philips (21.03%) scanners (Acquisition Plane=SAGITTAL; Acquisition Type=3D; Coil=PA; Field Strength=1.49399995803833 tesla; Flip Angle=8.0 degree; Manufacturer=SIEMENS; Matrix X=192.0 pixels; Matrix Y=192.0 pixels; Matrix Z=160.0 ; Mfg Model=Symphony; Pixel Spacing X=1.25 mm; Pixel Spacing Y=1.25 mm; Pulse Sequence=IR/GR; Slice Thickness=1.2004 mm; TE=3.60999 ms; TI=1000.0 ms; TR=3000.0 ms; Weighting=T1). (details regarding the ADNI MRI data acquisition protocol can be found on ADNI's official webpage: [adni.loni.usc.edu](http://adni.loni.usc.edu)) Sánchez-Reyna *et al.* [2020].

### 4.2 Datasets

The data used for the experiment produced by ADNI (AD Neuroimaging Initiative) is a longitudinal multicenter study designed to develop clinical, imaging, genetic, and biochemical biomarkers to detect and track Alzheimer's disease (AD). Magnetic resonance data is a component of the comprehensive set of data collected from ADNI participants. ADNI started in 2004, and to date, three different phases of ADNI have been carried out. Jack Jr *et al.* [2008]. The magnetic resonance (MRI) protocol evolved over these 3 phases. The main goal of ADNI is to determine if it is possible to combine PET, MRI, and other biological markers, neuropsychological and clinical assessments to measure AD progress. Determination of sensitive and specific markers of very early AD progression is intended to aid researchers and clinicians in developing new treatments, monitoring their effectiveness, and reducing the time and cost of clinical trials. ADNI MR images and quantitative numerical data are publicly available. All scans remain available for download by qualified users through the Image Data Archive on the website (<http://adni.loni.usc.edu>).

The dataset selected in ADNI (Alzheimer's Disease Neuroimaging Initiative) is the collection "MPR; GradWarp; B1 Correction; N3", because in this collection, we have the images volumetric measurements where a uniform linear adjustment has already been made in the images to remove noise generated by the magnetic resonance device. The data set is the size of 2603 volumetric images labeled with patients diagnosed with Alzheimer's disease (AD) and with cognitively normal patients (CN). The dataset is divided into 924 MRIs of healthy people and 1679 people diagnosed with AD. All MRIs are labeled with the diagnosis. The ages of patients range from 50 to 89 years old, divided into men and women. In the experiment, we will use all datasets. It is essential to highlight the dataset's diversity because we have this variation with men and women of different ages in this set.

The dataset was selected for this study because it is one of the most comprehensive and standardized repositories for Alzheimer's disease research. ADNI provides high-quality,

longitudinal 3D T1-weighted MRI scans acquired across multiple clinical sites under harmonized imaging protocols, ensuring consistency and reliability in model training and evaluation. Its wide adoption in the scientific community reinforces its role as a benchmark dataset for validating computational and deep learning approaches. For instance, Bieger *et al.* [2024] employed ADNI data to investigate the impact of brain atrophy on transcranial direct current stimulation, emphasizing the robustness, clinical relevance, and methodological rigor that the dataset offers. Similarly, using ADNI in this work ensures comparability with state-of-the-art studies, reproducibility of results, and a diverse set of labeled MRI volumes that support the development and assessment of CNN-based models for Alzheimer's disease detection.

### 4.3 Pre-processing

We used collaborative tools in the pre-processing step, as spatial normalization, registration, and segmentation techniques for magnetic resonance imaging (MRI). This step tends to use a target volume or model to facilitate processing, take advantage of previous information and define a standard coordinate system for analysis.

In neuroimaging literature, MNI-152 space (Atlas) coordinate system is often used as a standard model. Talairach coordinates, also known as Talairach space, are a three-dimensional coordinate system of the human brain, used to map the location of brain structures regardless of individual differences in brain size and overall shape. The figure 3 exemplifies the MNI-152 Atlas used Brett *et al.* [2001].

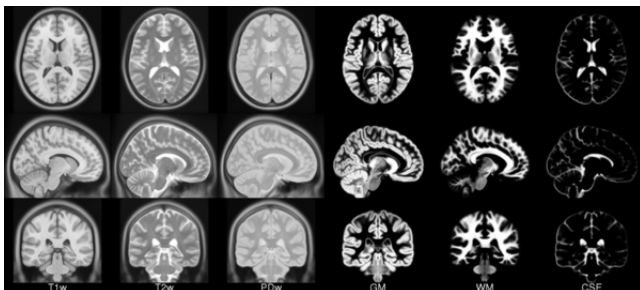


Figure 3. MNI-152

We used to process normalization and segmentation with MNI-152 Atlas the Advanced Normalization Tools (ANTs) Avants *et al.* [2009]. ANTs are useful for managing, interpreting, and viewing multidimensional data. ANTs are popularly considered an advanced medical image registration and segmentation toolkit.

The normalization procedure used (*antsRegistrationSyNQuick*) runs the symmetric image normalization method (SyN) to maximize the cross-correlation within the space of different maps and provides the Euler-Lagrange equations necessary for the optimization of the method normalization Avants *et al.* [2009]. The following snippet demonstrates an example of how the preprocessing script is used:

```
#!/bin/bash
bash antsRegistrationSyNQuick.sh -d 3 -f
  template_image.nii \
-m image_to_process.nii -t r -o output_prefix
```

We refer the reader to the ANTs documentation for further details about these parameters.<sup>1</sup>

Essentially, our brain extraction and normalization process involves the following steps:

- Winsorizing image intensities at the 1% and 99.9% quantiles;
- Bias field correction using the N4 algorithm, a variant of the well-known nonparametric nonuniform intensity normalization method (N3);
- Winsorizing image intensities again, this time at the 0.5% and 99.5% quantiles;
- Translation alignment using the center of mass;
- Rigid transformation (rotation and translation);
- Affine transformation (shearing and scaling);
- Symmetric diffeomorphic normalization (SyN), a non-linear transformation;
- Application of the atlas-based brain mask;
- Intensity normalization.

Winsorizing is a statistical transformation designed to minimize the influence of outliers. This is achieved by replacing extreme values with the closest values within a defined percentile range. According to Lusk, Halperin, and Heilig Lusk *et al.* [2011], the Winsorizing transformation was originally developed to “robustify” the sample mean, which is particularly sensitive to outliers.

To compute a Winsorized mean, one first sorts the dataset and replaces the smallest  $k$  values with the  $(k + 1)^{\text{th}}$  smallest value. The same is done for the largest  $k$  values, replacing them with the  $(k + 1)^{\text{th}}$  largest value. The mean of this modified dataset is then called the Winsorized mean. When the data come from a symmetric population, the Winsorized mean provides a robust and unbiased estimate of the population mean.

Normalization performs a rigid transformation commonly called Euclidean transformation Tustison *et al.* [2013]. Rigid transformations include rotations, translations, reflections, or their combination. Sometimes reflections are excluded from the definition of a rigid transformation, imposing that the transformation also preserves the laterality of the figures in Euclidean space. Any object will retain the same shape and size after a Euclidean transformation. Normalization also performs an affine transformation, or an affinity, which is nothing more than a geometric transformation that preserves lines and parallelism Avrithis *et al.* [2001].

The Medical Imaging NetCDF Toolkit (MINC-TOOLKIT) was also used in the segmentation process. The MINC file format, libraries, and tools provide a framework for manipulating medical images regardless of the modality. MINC 1.0 was created in 1993 to meet the needs of the brain imaging research community Vincent *et al.* [2016]. The format is extremely flexible, providing various types of voxel data, arbitrary dimensions, and a rich set of supporting data. New functionality and data fields can be added to the specification without modifying existing files or software. MINC 1.0 files define a “voxel” coordinate system and a transformation to a “world” or stereotaxic coordinate system. Voxel data can

<sup>1</sup><https://github.com/ANTsX/ANTs>

include an optional range conversion from one entire storage format to a floating-point memory format Vincent *et al.* [2004]. To perform the segmentation process, it was necessary to convert MRI in NIFTI format (.nii) to extension (.mnc) to use MINC (minc-toolkit). The mask was then applied to remove the brain skull image that is not necessary for our analysis context of Alzheimer's disease. In the figure 4, we have the mask used in the segmentation process.

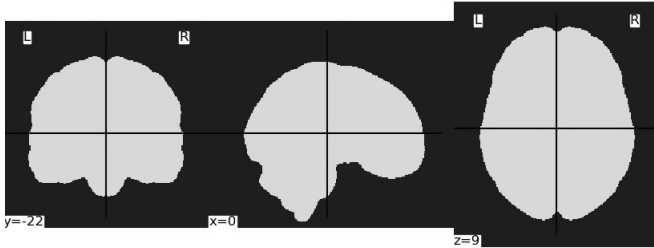


Figure 4. Example mask atlas

And the figure 5 shows a segmented and normalized image in 2D format only for demonstration in this article. You can see that in figure 3, the image is already in a format that will be used in the training of the classifier; the normalization process was necessary since the images in their original format had different positions, so we decided to adjust the position and angle we used. After pre-processing, each MRI had dimensions of  $79 \times 95 \times 79$ . Before processing, it had dimensions of  $224 \times 224 \times 224$ . We can observe a significant reduction, with non-essential parts for diagnosing AD being removed. Pre-processed images were used to conduct the experiments.



Figure 5. Segmented and Normalized Image

#### 4.4 Methodology

This subsection details the overall methodology adopted in this study for detecting Alzheimer's disease using convolutional neural networks (CNNs). The proposed pipeline includes the acquisition of 3D MRI images, preprocessing steps to ensure spatial consistency, model selection, and evaluation.

Initially, all MRI volumes underwent spatial normalization and skull-stripping to standardize dimensions and remove irrelevant anatomical features. These steps were essential to minimize input variance and reduce computational complexity.

The experiments were divided into two core approaches: the use of 2D CNNs on individual slices and 3D CNNs applied to entire volumetric data. Both architectures were evaluated

under the same training conditions, including optimization settings, data splitting strategy (hold-out), and hardware.

This methodological design aimed to compare how dimensionality and model depth affect classification performance, while maintaining consistency in preprocessing and data input. The use of standardized anatomical space (MNI-152) and registration techniques ensured that the CNNs learned from comparable anatomical regions across all samples.

The implementation of the proposed deep learning models was carried out using the Python programming language, which offers extensive libraries and tools for scientific computing and machine learning. Specifically, the Keras library—built on top of TensorFlow—was employed to construct, train, and evaluate the convolutional neural network (CNN) architectures. Keras provides a high-level, user-friendly API that facilitated rapid prototyping and experimentation while maintaining compatibility with GPU acceleration. All preprocessing steps, model configuration, and training procedures were executed within this Python-based environment.

#### 4.5 Model validation

To validate both the 2D and 3D CNN models, we adopted the hold-out method. This approach consists of partitioning the dataset into two distinct subsets: a training set and a test set, as described by Yadav and Shukla [2016]. The training set is used to fit the model, while the test set is employed to evaluate its performance on previously unseen data, in accordance with Nam *et al.* [2021]. In this study, a commonly used split was applied, with 80% of the data allocated for training and the remaining 20% reserved for testing.

Model performance was evaluated using Accuracy, Precision, and Recall (Sensitivity) as the primary metrics. Accuracy measures the proportion of correctly classified samples, while Precision quantifies the ratio of true positive predictions to the total number of positive predictions. Recall, also referred to as Sensitivity, evaluates the model's ability to correctly identify positive instances. In addition, a confusion matrix was employed to provide a detailed analysis of classification results by summarizing true positives, true negatives, false positives, and false negatives.

The hold-out method is particularly suitable for scenarios involving large datasets, limited computational time, or the early stages of model development in data science projects, as discussed by Dwork *et al.* [2015].

#### 4.6 CNN 2D Model

For this approach, 2D CNNs have the ability to extract AD-related discriminative features, such as brain shrinkage, from each image slice, and classification of each subject is conducted based on the image slices of that subject. Figure 6 indicates our single-view 2D CNN structure. Single-view (coronal, sagittal and axial) image slices of all subjects in the training set are used to train a 2D CNN. For testing, all image slices of an MRI scan are then classified by the CNN model. The final classification is determined by a majority voting strategy on all image slices.

Some studies 2D that conducted similar training for Alzheimer's Disease (AD) detection utilized Long Short-Term Memory (LSTM), a variant of Recurrent Neural Networks (RNN). LSTMs are particularly effective in processing sequential data, such as time series and medical images organized in sequences Ebrahimi-Ghahnavieh *et al.* [2019]. This is due to their ability to store and access information over extended periods, overcoming the limitations of traditional RNNs, which are prone to vanishing or exploding gradient problems. These studies have shown that applying LSTM can complement CNN-based approaches, providing significant improvements in the analysis and classification of patterns associated with AD Dua *et al.* [2020].

However, this approach using RNN requires categorizing the coronal, sagittal and axial image slices, as well as having to save the results to an LSTM after CNN processing. This makes the process more complex. For this article, we chose to carry out a simpler experiment, using MRI pre-processing techniques and comparing the classification in the 2D and 3D CNN network models.

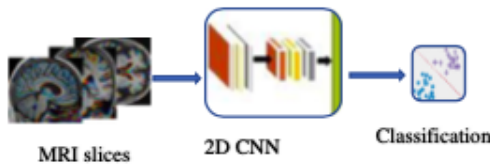


Figure 6. 2D CNN Model

Table 2. Comparison of 2D CNN Network Architectures

Network	Epoch	#Layers	#Conn	Image Inp Size	Acc(%)
LeNet-5	10	5	15	$128 \times 128 \times 1$	81.22
AlexNet	10	5	24	$128 \times 128 \times 1$	64.12
SqueezeNet	10	20	78	$128 \times 128 \times 1$	69.49
GoogLeNet	10	16	46	$128 \times 128 \times 1$	71.42
ResNet-18	10	94	349	$128 \times 128 \times 1$	<b>90.17</b>
ResNet-50	10	53	192	$128 \times 128 \times 1$	74.46

## 4.7 CNN 3D Model

The preprocessed MRI datasets (ADNI) were used to train 3D CNNs for voxel-based decision-making. As noted in Table 2, 3D CNNs have a significantly larger number of learnable parameters, making their training computationally intensive. Despite this challenge, we opted to use these deep models to enable a direct comparison with 2D CNNs.

To construct the 3D CNNs, we extended the 2D filters of certain CNN models listed in Table 1 into the third dimension, creating 3D filters. Additionally, other layers described in Section 2.1 were adjusted to align with these new filters. Training 3D CNNs introduces complexities due to the increased number of learnable parameters compared to their 2D counterparts, often making the backpropagation process more difficult to converge, especially when training from scratch.

To address this issue, we transferred the learnable parameters from pretrained 2D CNNs (trained on ADNI dataset MRI)

to 3D CNNs. This was achieved by duplicating the 2D filters along the third dimension, effectively transforming them into 3D filters. This approach is feasible because MRI scans can be represented as sequences of image slices. To the best of our knowledge, the application of transfer learning with 3D CNNs has not been previously explored for classification tasks.

During training, the 3D CNNs are expected to capture AD-related features within each MRI slice and recognize patterns across the slices. Table 2 lists the 3D models used in our study, along with their number of learnable parameters and memory requirements. As the filter dimensions increase, so does the number of parameters. A diagram illustrating the architecture of our 3D CNNs is presented in Figure 7.

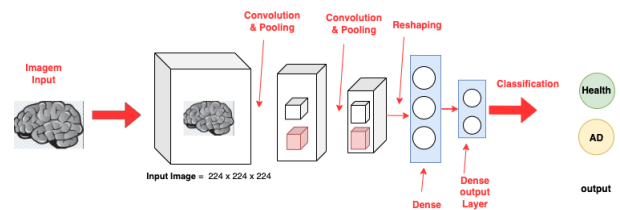


Figure 7. 3D CNN Model

Table 3. Comparison of 3D CNN Network Architectures

Network	Epoch	Layers	Image Input Size	Acc(%)
LeNet-5	10	5	$193 \times 229 \times 193$	82.33
ResNet-18	10	8	$193 \times 229 \times 193$	<b>87.88</b>
ResNet-50	10	18	$193 \times 229 \times 193$	84.65

The input images used in this study were obtained from the ADNI dataset and have dimensions of  $193 \times 229 \times 193$  voxels. These dimensions correspond to the width, height, and depth of each 3D MRI volume, respectively. The third dimension represents the voxel-wise depth of the brain scan, capturing the internal structure along the sagittal, coronal, or axial planes depending on the orientation. In the context of Alzheimer's disease detection, this depth dimension is essential, as it preserves the volumetric integrity of the brain and enables convolutional neural networks to learn spatial patterns associated with neurodegeneration across multiple slices. Processing the entire volume as a 3D input allows the model to capture relevant features not only in individual slices but also in the relationships between slices throughout the brain structure. In the table 4 we define input size.

Table 4. MRI image dimensions and anatomical meaning (ADNI dataset)

Position	Dimension	Description
[0]	193	Depth (Z) – number of axial slices
[1]	229	Height (Y) – superior-inferior direction
[2]	193	Width (X) – left-right direction

## 5 Results and Discussion

As previously mentioned, this study utilized the ADNI dataset. For our experiments, we employed a dataset consisting of

2,603 labeled volumetric MRI images, including patients diagnosed with Alzheimer's disease (AD) and cognitively normal (CN) individuals. Specifically, the dataset comprises 924 MRI scans from cognitively normal participants and 1,679 scans from individuals diagnosed with AD. Each MRI scan is labeled according to the patient's diagnosis. The patients' ages range from 50 to 89 years, with a balanced distribution between men and women. This dataset was chosen because it had undergone preprocessing and correction during image acquisition, ensuring its reliability for analysis.

The MRI dataset was not properly balanced, which may affect the quality and reliability of the analyses performed. This imbalance occurs when there is an unequal distribution between the classes or categories of interest, such as specific pathologies, age groups, or genders, leading to biases in predictive models. Consequently, the model's performance may be compromised, favoring more represented classes while neglecting those with less representation.

The same training parameters were used for 2D CNN that contained mini-batch size = 64, initial learning rate = 0.0003, max-pooling= 2 and L2 regularization = 0.0005. Stochastic gradient descent (SGD) with momentum 1/4 0.9 was the optimizer algorithm with early stopping according to the validation set. However, mini-batch size 1/4 8 was used for 3D CNNs because of the available computational resources.

All experiments were conducted using the following hardware configuration, 2 x (Intel Xeon E5-2650 v3 Haswell (Q3'14), 2.3 GHz) with 20 cores (10 per CPU), totaling 100 cores and 200 threads 128 GB DDR4 RAM, 2 x (NVIDIA Tesla K80, Kepler, 2 x 2496 CUDA Threads) of GPU memory and all deep learning models were implemented using Python programming language using Keras and TensorFlow (v.1.15). The training durations of various CNNs and approaches are presented in 8.

The entire set of preprocessed MRIs was used to train 3D CNNs, enabling voxel-based decision-making. As shown in Table 3, 3D CNNs involve a large number of learnable parameters, making their training computationally intensive. Despite this, we employed these deep models to facilitate a comparison with 2D CNNs. To construct the 3D CNNs, we extended the 2D filters of certain CNN models listed in Table 2 into the third dimension, thereby creating 3D filters. All models have the same training parameters, except mini-batch size, 64 for 2D CNNs and 8 for 3D CNNs. The models were trained using the same hardware and software resources.

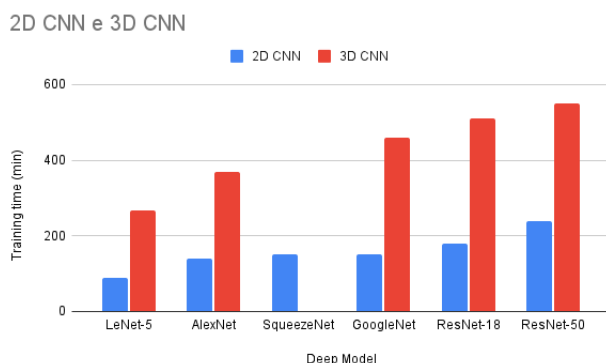


Figure 8. Training time for each model

Overall, ResNet-18 and LeNet-5 demonstrated the best performance on our dataset (ADNI). In the 2D CNN ResNet-18 model, without resizing the images after pre-processing, an accuracy of 90.17% was achieved. Similarly, LeNet-5 produced good results, albeit with a smaller input size. For the 3D CNN ResNet-18 model, using an image input size of  $79 \times 95 \times 79$ , without reducing the input dimensions, an accuracy of 87.88% was obtained. However, the 2D model achieved better accuracy, reaching 90.17%, while the 3D model achieved an accuracy of 87.88%. As mentioned above, we used the hold-out method to validate the models, since the ADNI dataset contains a large volume of images. These findings suggest that the two-dimensional approach was more effective for the proposed task, although both techniques proved to be suitable for data analysis. The Figure 9 shows the loss function graph for the ResNet-18 3D model, indicating the evolution of the training over the epochs.

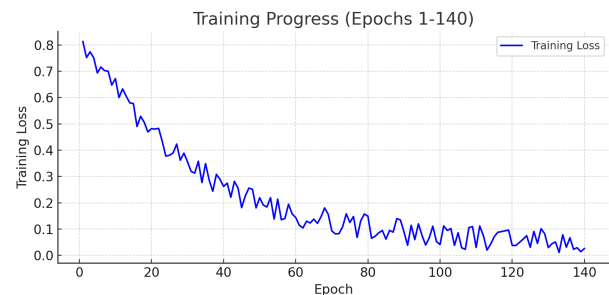


Figure 9. Training loss for 3D ResNet-18

## 6 Conclusions

This paper discusses the design, implementation, and experimentation of several CNN-based approaches for MRI-based Alzheimer's Disease (AD) detection. In the initial approach, a 2D CNN was trained on MRI slices in a single-view mode. For classification, the model evaluated all slices of a patient from a specific view to make its decision. In the second approach, a 3D CNN was employed to classify MRI volumes, each in a single decision.

Pre-processing the images using the MNI-152 (Atlas) spatial coordinate system was fundamental to improving the results obtained. This process made it possible to remove regions of the brain that are not relevant for detecting Alzheimer's, focusing only on the areas of greatest interest for diagnosis. Standardization based on MNI-152 helped to reduce noise and highlight significant brain structures, optimizing the performance of the deep learning models used in the study and directly contributing to greater accuracy in the analyses carried out.

In this study, I believe that one of the great differentials of this article is the use of pre-processing with Atlas MNI-152, which allows the removal of parts of the images that are not essential for the diagnosis of Alzheimer's Disease (AD). This approach helps to reduce the volume of data processed, focusing only on the relevant regions of the brain, which can improve the accuracy and efficiency of classification models, as well as simplifying the process of training neural networks.

While deep learning methods show strong potential for accurate AD detection, training 3D CNNs from scratch delivered suboptimal results on our MRI dataset. A notable challenge lies in the reliance on large datasets, which is a significant limitation of these approaches. Furthermore, the imbalance in the ADNI dataset adversely affected the outcomes. Future work should focus on utilizing balanced datasets to improve the reliability and robustness of the models.

## 7 Future Work

Future research will focus on a multi-faceted expansion of the current framework. Initially, we intend to conduct a more granular hyperparameter optimization, specifically targeting the depth and configuration of convolutional layers to maximize performance metrics. Beyond architectural refinements, we will transition from whole-brain analysis to ROI-centric approaches using segmented MRI images. By isolating clinically relevant brain regions, we aim to enhance the feature discrimination capabilities of our CNN models.

To address the inherent challenges of medical datasets, subsequent investigations will implement data balancing techniques and transition from binary to multiclass classification to distinguish between various stages of Alzheimer's Disease progression. We also propose the integration of heterogeneous data sources and multimodal fusion (e.g., PET and CT scans) to improve model generalizability.

Furthermore, we will explore Federated Learning (FL) to facilitate multi-institutional collaboration while maintaining strict patient privacy. Finally, we intend to investigate ensemble learning strategies and collaborate with neuroscience specialists to ensure that the learned features align with established clinical biomarkers, ultimately improving the stability and diagnostic accuracy of the proposed models.

## Declarations

### Authors' Contributions

Augusto Berwaldt de Oliveira conducted the research, developed the methodology, and carried out the experiments and data analysis. Claudio Resin Geyer contributed by revising the manuscript and providing critical feedback throughout the development of the work. All authors participated in the conception of the approach and approved the final version of the manuscript.

### Competing interests

The authors declare that they have no competing interests.

### Acknowledgements

Data collection and sharing for this project were funded by the Alzheimer's Disease Neuroimaging Initiative (ADNI), National Institutes of Health (Grant No. U01 AG024904), and DOD ADNI (Department of Defense Award No. W81XWH-12-2-0012). ADNI is funded by the National Institute on Aging (NIA), the National Institute of Biomedical Imaging and Bioengineering (NIBIB), and generous contributions from the following: AbbVie, Alzheimer's Associ-

ation; Alzheimer's Drug Discovery Foundation. The Canadian Institutes of Health Research provide funds to support ADNI clinical sites in Canada. Private sector contributions are facilitated by the Foundation for the National Institutes of Health (<https://www.fnih.org>). The grantee organization is the Northern California Institute for Research and Education, and the study is coordinated by the Alzheimer's Therapeutic Research Institute at the University of Southern California. ADNI data are disseminated by the Laboratory of Neuro Imaging (LONI) at the University of Southern California. Department of Pharmacology, - UFRGS, Porto Alegre, RS, BRZimmer Lab (<http://www.zimmer-lab.org>)

### Funding

This research received no external funding and was fully supported by the author.

### Availability of data and materials

The dataset used in this study is available at: <https://adni.loni.usc.edu>, and the script used for training can be accessed at: <https://gist.github.com/augustoberwaldt/50b46be801281c4b3b0d04a8a8b0817f>.

## References

- Avants, B. B., Tustison, N., and Song, G. (2009). Advanced normalization tools (ants). *Insight j*, 2(365):1–35.
- Avrithis, Y., Xirouhakis, Y., and Kollias, S. (2001). Affine-invariant curve normalization for object shape representation, classification, and retrieval. *Machine Vision and Applications*, 13:80–94.
- Bhatt, D., Patel, C., Talsania, H., Patel, J., Vaghela, R., Pandya, S., Modi, K., and Ghayvat, H. (2021). Cnn variants for computer vision: History, architecture, application, challenges and future scope. *Electronics*, 10(20):2470.
- Bieger, A., Brum, W. S., Borelli, W. V., Therriault, J., De Bastiani, M. A., Moreira, A. G., Benedet, A. L., Ferrari-Souza, J. P., Da Costa, J. C., Souza, D. O., et al. (2024). Influence of different diagnostic criteria on alzheimer disease clinical research. *Neurology*, 103(5):e209753.
- Billones, C. D., Demetria, O. J. L. D., Hostallero, D. E. D., and Naval, P. C. (2016). Demnet: a convolutional neural network for the detection of alzheimer's disease and mild cognitive impairment. In *2016 IEEE region 10 conference (TENCON)*, pages 3724–3727. IEEE.
- Brett, M., Christoff, K., Cusack, R., Lancaster, J., et al. (2001). Using the talairach atlas with the mni template. *Neuroimage*, 13(6):85–85.
- Bringas, S., Salomón, S., Duque, R., Lage, C., and Montaña, J. L. (2020). Alzheimer's disease stage identification using deep learning models. *Journal of Biomedical Informatics*, 109:103514.
- Carcagni, P., Leo, M., Cuna, A., Mazzeo, P. L., Spagnolo, P., Celeste, G., and Distante, C. (2019). Classification of skin lesions by combining multilevel learnings in a densenet architecture. In *Image Analysis and Processing—ICIAP 2019: 20th International Conference, Trento, Italy*,

- September 9–13, 2019, *Proceedings, Part I 20*, pages 335–344. Springer.
- Chauhan, R., Ghanshala, K. K., and Joshi, R. (2018). Convolutional neural network (cnn) for image detection and recognition. In *2018 first international conference on secure cyber computing and communication (ICSCCC)*, pages 278–282. IEEE.
- Dorfner, F. J., Patel, J. B., Kalpathy-Cramer, J., and ... (2025). A review of deep learning for brain tumor analysis in mri. *NPJ Precision Oncology*. DOI: 10.1038/s41698-024-00789-2.
- Dua, M., Makhija, D., Manasa, P., and Mishra, P. (2020). A cnn-rnn-lstm based amalgamation for alzheimer's disease detection. *Journal of Medical and Biological Engineering*, 40(5):688–706.
- Dwork, C., Feldman, V., Hardt, M., Pitassi, T., Reingold, O., and Roth, A. (2015). The reusable holdout: Preserving validity in adaptive data analysis. *Science*, 349(6248):636–638.
- Ebrahimi-Ghahnavieh, A., Luo, S., and Chiong, R. (2019). Transfer learning for alzheimer's disease detection on mri images. In *2019 IEEE International Conference on Industry 4.0, Artificial Intelligence, and Communications Technology (IAICT)*, pages 133–138. IEEE.
- Ebrahimighahnavieh, M. A., Luo, S., and Chiong, R. (2020). Deep learning to detect alzheimer's disease from neuroimaging: A systematic literature review. *Computer methods and programs in biomedicine*, 187:105242.
- Feng, C., Elazab, A., Yang, P., Wang, T., Zhou, F., Hu, H., Xiao, X., and Lei, B. (2019). Deep learning framework for alzheimer's disease diagnosis via 3d-cnn and fsbi-lstm. *IEEE Access*, 7:63605–63618.
- Guo, Y. (2017). Deep learning for visual understanding.
- Guo, Y., Li, Q., Yang, X., Jaffee, M. S., Wu, Y., Wang, F., and Bian, J. (2022). Prevalence of alzheimer's and related dementia diseases and risk factors among transgender adults, florida, 2012–2020. *American Journal of Public Health*, 112(5):754–757.
- Hao, W., Yizhou, W., Yaqin, L., and Zhili, S. (2020). The role of activation function in cnn. In *2020 2nd International Conference on Information Technology and Computer Application (ITCA)*, pages 429–432. IEEE.
- He, K., Zhang, X., Ren, S., and Sun, J. (2016). Deep residual learning for image recognition. In *Proceedings of the IEEE conference on computer vision and pattern recognition*, pages 770–778.
- Irfansyah, D., Mustikasari, M., and Suroso, A. (2021). Arsitektur convolutional neural network (cnn) alexnet untuk klasifikasi hama pada citra daun tanaman kopi. *Jurnal Informatika: Jurnal Pengembangan IT*, 6(2):87–92.
- Jack Jr, C. R., Bernstein, M. A., Fox, N. C., Thompson, P., Alexander, G., Harvey, D., Borowski, B., Britson, P. J., L. Whitwell, J., Ward, C., et al. (2008). The alzheimer's disease neuroimaging initiative (adni): Mri methods. *Journal of Magnetic Resonance Imaging: An Official Journal of the International Society for Magnetic Resonance in Medicine*, 27(4):685–691.
- Karwath, A., Hubrich, M., Kramer, S., and Initiative, A. D. N. (2017). Convolutional neural networks for the identification of regions of interest in pet scans: a study of representation learning for diagnosing alzheimer's disease. In *Conference on Artificial Intelligence in Medicine in Europe*, pages 316–321. Springer.
- Kayed, M., Anter, A., and Mohamed, H. (2020). Classification of garments from fashion mnist dataset using cnn lenet-5 architecture. In *2020 international conference on innovative trends in communication and computer engineering (ITCE)*, pages 238–243. IEEE.
- Kazemi, Y. and Houghten, S. (2018). A deep learning pipeline to classify different stages of alzheimer's disease from fmri data. In *2018 IEEE Conference on Computational Intelligence in Bioinformatics and Computational Biology (CIBCB)*, pages 1–8. IEEE.
- Lakhan, A., Grønli, T.-M., Muhammad, G., and Tiwari, P. (2023). Edcnns: Federated learning enabled evolutionary deep convolutional neural network for alzheimer disease detection. *Applied Soft Computing*, 147:110804.
- Lakhan, A., Mohammed, M. A., Abd Ghani, M. K., Abdulkaareem, K. H., Marhoon, H. A., Nedoma, J., Martinek, R., and Deveci, M. (2024). Fdcnn-as: Federated deep convolutional neural network alzheimer detection schemes for different age groups. *Information Sciences*, 677:120833.
- Litjens, G., Kooi, T., Bejnordi, B. E., Setio, A. A. A., Ciompi, F., Ghafoorian, M., Van Der Laak, J. A., Van Ginneken, B., and Sánchez, C. I. (2017). A survey on deep learning in medical image analysis. *Medical image analysis*, 42:60–88.
- Liu, K., Kang, G., Zhang, N., and Hou, B. (2018). Breast cancer classification based on fully-connected layer first convolutional neural networks. *IEEE Access*, 6:23722–23732.
- Lopes, F. et al. (2024). Hybrid approaches to address class imbalance in medical imaging. *Journal of Medical Imaging and Analysis*. under review/preprint or speculative source.
- Lusk, E. J., Halperin, M., and Heilig, F. (2011). A note on power differentials in data preparation between trimming and winsorizing. *Business Management Dynamics*, 1(2):23.
- Mesran, M., Yahya, S. R., Nugroho, F., Windarto, A. P., et al. (2024). Investigating the impact of relu and sigmoid activation functions on animal classification using cnn models. *Jurnal RESTI (Rekayasa Sistem dan Teknologi Informasi)*, 8(1):111–118.
- Muhammad, U., Wang, W., Chattha, S. P., and Ali, S. (2018). Pre-trained vggnet architecture for remote-sensing image scene classification. In *2018 24th International Conference on Pattern Recognition (ICPR)*, pages 1622–1627. IEEE.
- Mutasa, S., Sun, S., and Ha, R. (2021). Understanding artificial intelligence based radiology studies: Cnn architecture. *Clinical Imaging*, 80:72–76.
- Nam, Y., Arai, Y., Kunizane, T., and Koizumi, A. (2021). Water leak detection based on convolutional neural network using actual leak sounds and the hold-out method. *Water Supply*, 21(7):3477–3485.
- Pradhan, N., Sagar, S., and Jagadesh, T. (2024). Advance convolutional network architecture for mri data investigation for alzheimer's disease early diagnosis. *SN Computer Science*, 5(1):167.
- Qin, Z., Liu, Z., and Zhu, P. (2022). Aiding alzheimer's disease diagnosis using graph convolutional networks based

- on rs-fmri data. In *2022 15th International Congress on Image and Signal Processing, BioMedical Engineering and Informatics (CISP-BMEI)*, pages 1–7. IEEE.
- Salmi, M. et al. (2024). Handling imbalanced medical datasets: A review of a decade of research. *Artificial Intelligence Review*, 57. DOI: 10.1007/s10462-024-10884-2.
- Sánchez-Reyna, A. G., Espino-Salinas, C. H., Rodríguez-Aguayo, P. C., Salinas-Gonzalez, J. D., Zanella-Calzada, L. A., Martínez-Escobar, E. Y., Celaya-Padilla, J. M., Galván-Tejada, J. I., Galván-Tejada, C. E., and Initiative, A. D. N. (2020). Feature selection and machine learning applied for alzheimer's disease classification. In *VIII Latin American Conference on Biomedical Engineering and XLII National Conference on Biomedical Engineering: Proceedings of CLAIB-CNIB 2019, October 2-5, 2019, Cancún, México*, pages 121–128. Springer.
- Shen, D., Wu, G., and Suk, H.-I. (2017). Deep learning in medical image analysis. *Annual review of biomedical engineering*, 19(1):221–248.
- Sulam, J., Aberdam, A., Beck, A., and Elad, M. (2019). On multi-layer basis pursuit, efficient algorithms and convolutional neural networks. *IEEE transactions on pattern analysis and machine intelligence*, 42(8):1968–1980.
- Szegedy, C., Ioffe, S., Vanhoucke, V., and Alemi, A. (2017). Inception-v4, inception-resnet and the impact of residual connections on learning. In *Proceedings of the AAAI conference on artificial intelligence*, volume 31.
- Szegedy, C., Liu, W., Jia, Y., Sermanet, P., Reed, S., Anguelov, D., Erhan, D., Vanhoucke, V., and Rabinovich, A. (2015). Going deeper with convolutions. In *Proceedings of the IEEE conference on computer vision and pattern recognition*, pages 1–9.
- Tolias, G., Sicre, R., and Jégou, H. (2015). Particular object retrieval with integral max-pooling of cnn activations. *arXiv preprint arXiv:1511.05879*.
- Tustison, N. J., Avants, B. B., Cook, P. A., Song, G., Das, S., van Strien, N., Stone, J. R., and Gee, J. C. (2013). The ants cortical thickness processing pipeline. In *Medical Imaging 2013: Biomedical Applications in Molecular, Structural, and Functional Imaging*, volume 8672, page 86720K. International Society for Optics and Photonics.
- Vincent, R. D., Janke, A., Sled, J. G., Baghdadi, L., Neelin, P., and Evans, A. C. (2004). Minc 2.0: a modality independent format for multidimensional medical images. In *10th Annual Meeting of the Organization for Human Brain Mapping*, volume 2003, page 2003.
- Vincent, R. D., Neelin, P., Khalili-Mahani, N., Janke, A. L., Fonov, V. S., Robbins, S. M., Baghdadi, L., Lerch, J., Sled, J. G., Adalat, R., et al. (2016). Minc 2.0: a flexible format for multi-modal images. *Frontiers in neuroinformatics*, 10:35.
- Wolterink, J. M., Leiner, T., Viergever, M. A., and Isgum, I. (2017). Automatic segmentation and disease classification using cardiac cine mr images. *ArXiv*. arXiv:1708.01141.
- Wu, H. and Gu, X. (2015). Max-pooling dropout for regularization of convolutional neural networks. In *Neural Information Processing: 22nd International Conference, ICONIP 2015, Istanbul, Turkey, November 9-12, 2015, Proceedings, Part I 22*, pages 46–54. Springer.
- Yadav, S. and Shukla, S. (2016). Analysis of k-fold cross-validation over hold-out validation on colossal datasets for quality classification. In *2016 IEEE 6th International conference on advanced computing (IACC)*, pages 78–83. IEEE.
- Yu, W., Yang, K., Yao, H., Sun, X., and Xu, P. (2017). Exploiting the complementary strengths of multi-layer cnn features for image retrieval. *Neurocomputing*, 237:235–241.
- Zafar, A., Aamir, M., Mohd Nawi, N., Arshad, A., Riaz, S., Alruban, A., Dutta, A. K., and Almotairi, S. (2022). A comparison of pooling methods for convolutional neural networks. *Applied Sciences*, 12(17):8643.
- Zhang, H. and Qie, Y. (2023). Applying deep learning to medical imaging: A review. *Applied Sciences*, 13(18):10521. DOI: 10.3390/app131810521.